

On the nature of the Fermi GeV excess: leptonic outbursts from the past Galactic center activity

Francesca Calore*

GRAPPA, University of Amsterdam, Science Park 904, 1098XH, Amsterdam, Netherlands

E-mail: f.calore@uva.nl

on behalf of I. Cholis, C. Evoli, D. Hooper, T. Linden and C. Weniger

We scrutinize the possibility that cosmic-ray leptonic outbursts give origin to the *Fermi* Galactic center GeV excess, whose spectral and morphological properties have been recently re-assessed in light of background model systematics in the inner region of the Milky Way. We demonstrate that the gamma-ray emission from leptonic cosmic rays interacting with gas and ambient photons and injected during past outburst events might explain the excess features, albeit under specific assumptions on burst properties (age and spectral injection index) and propagation conditions. This contribution is based on Ref. [1].

*The 34th International Cosmic Ray Conference,
30 July- 6 August, 2015
The Hague, The Netherlands*

*Speaker.

1. Introduction

Since 2009, a spatially extended excess of gamma rays collected by the Large Area Telescope (LAT), aboard the *Fermi* satellite, from the inner region of the Milky Way has been claimed by different and independent groups, see for example [2, 3, 4, 5, 6, 7]. Recently, Ref. [6] re-assessed the spectral and morphological properties of this excess emission, robustly characterizing the signal against systematic uncertainties related to the high density of cosmic rays (CR), gas, magnetic fields and abundance of point sources within the region $|l| < 20^\circ$ and $2^\circ < |b| < 20^\circ$. The systematic uncertainties due to the Galactic diffuse emission modeling were derived through an innovative method based on a *principal component analysis* of residuals along the Galactic plane (please refer to [6] for more details). The systematic uncertainties are fully encoded in a covariance matrix whose effect in the fit can be interpreted as the result of the variation of slope and normalisation of the Galactic diffuse emission components within the uncertainties allowed by the gamma-ray data (see Refs. [6, 8] for more details). The excess properties in light of background model systematics are significantly different from what was claimed before and allow more freedom for models fitting the excess, as it has been shown in Ref. [8] in the case of dark matter annihilation models. Given the striking similarity that the excess data shows with the expected gamma-ray signal from dark matter particles annihilating in the Milky Way, there has been a great excitement in interpreting the GeV excess in terms of annihilating dark matter, see for example [5, 4, 8, 9, 10]. However, also non-dark-matter astrophysical interpretations have been proposed. Besides the possibility that the excess arises from a population of dim, unresolved, point-sources (as recently strongly supported by Ref. [11, 12]), the excess emission can originate from a high-energy population of CR electrons injected in the past at the Galactic center (GC) and leading to gamma rays through inverse Compton scattering (ICS) and bremsstrahlung emission.¹ Such a promising scenario was proposed by Ref. [14] and it finds support from existing hints on the past activity of the GC, above all the presence of the *Fermi* bubbles [15, 16, 17], that might originate either from outflows of the massive central black hole or from starburst events of the central nuclear stellar cluster.

We here present a systematic study of the CR leptonic outburst scenario, by evaluating whether and under what circumstances it can indeed explain the GeV excess observed features.

2. A series of leptonic outbursts from the Galactic center

Ref. [14] showed that the gamma-ray flux derived by diffusion and energy losses of a population of high-energy electrons injected at the GC about 1 Myr ago might explain the spectrum and morphology of the observed GeV excess. However, a systematic study of this scenario and the exploration of a large parameter space for the CR propagation conditions was lacking. In Ref. [1], we simulate the propagation of electrons in the inner Galaxy region through the publicly available numerical codes *Galprop* [18] and *DRAGON* [19, 20].

The high-energy electrons are injected in the interstellar medium at a given time in the past and their propagation is followed in time steps until today, by solving the propagation equation that

¹In principle, also CR proton injection leads to gamma rays through neutral pion production. However, hadronic scenarios predict gamma-ray signals correlated with the gas distribution in the Galactic disk and thus incompatible with the observed characteristics of the excess [13].

accounts for diffusion, convection, re-acceleration and energy losses. We assume that electrons are injected homogeneously within a cylinder of 50 pc radius and 100 pc height around the GC. The primary injection spectrum is a power-law with exponential cutoff:

$$\frac{dN_e}{dE_e} = \mathcal{N} E_e^{-\alpha} \exp\{-E_e/E_{\text{cut}}\} \quad (2.1)$$

where \mathcal{N} is a normalization factor related to the total injected energy ($\sim 10^{51}$ erg) that we will allow to vary freely in the fit to the observed GeV excess data. The spectral index ranges in the interval $\alpha = 1 - 3$, while the cutoff energies in the range 15 – 100 GeV (or higher for the single burst models). The injection spectrum is thus the spectrum of electrons at ~ 50 pc from the GC, and not necessarily the spectrum at the source.

The CR propagation model is the standard `Galprop` setup, with homogeneous diffusion (described by D_0 and δ), convection (perpendicular to the Galactic disk dv_c/dz) and re-acceleration (v_A) included. Synchrotron energy losses depend on the structure of the magnetic field, whose spatial distribution is assumed to be an exponential in both r and z with parameters B_0 (the magnetic field intensity at the GC), r_c and z_c (the characteristic scale lengths). ICS is instead determined by the Interstellar Radiation Field (ISRF) model. We use the model provided by `Galprop v54` [21] and we allow for the normalizations of the optical and infrared components to vary. The distribution of interstellar atomic hydrogen (HI) and molecular hydrogen (H_2) are the ones provided by `Galprop v54`. Finally, when simulating the outburst with `DRAGON`, we also account for inhomogeneous and/or anisotropic propagation, parameterized by two diffusion coefficients, D_{xx} and D_{zz} , that represent the diffusion parallel to and perpendicular to the Galactic disk, respectively.

Gamma rays from the primary electron population are produced by ICS off the ISRF photons and by bremsstrahlung off the interstellar gas [22].

We compare the ensuing gamma-ray fluxes with the GeV excess spectral and morphological properties as observed by Ref. [6] in the region of interest (ROI) $|\ell| < 20^\circ$ and $2^\circ < |b| < 20^\circ$, fully accounting for the systematic uncertainties due to foreground variations. In particular, Ref. [6] derived the morphology of the GeV excess in ten sub-regions of the main ROI, characterizing spectrum and systematic uncertainties of the excess in each of the ten sub-regions.

We perform a fit of the predicted model spectra to the GeV excess data in the ten sub-regions simultaneously by minimizing the combined χ^2 :

$$\chi^2 = \sum_{i=1}^{10} \sum_{j,k=1}^{24} (d_{ij} - \mu_{ij})(\Sigma_{jk}^i)^{-1} (d_{ik} - \mu_{ik}), \quad (2.2)$$

where d_{ij} and μ_{ij} are the measured and predicted flux in the sub-region i and energy bin j . The covariance matrix, Σ_{jk}^i , is defined for the energy bins j and k in the sub-region i . The χ^2 is assumed to follow a χ_k^2 distribution with $k = 240 - 1$ degrees of freedom, where the parameter of the model left free in the fitting procedure is the normalization \mathcal{N} .

3. Results

In Ref. [1], we set under scrutiny the leptonic outburst model by, firstly, performing a Bayesian scan over CR propagation parameters and burst properties for the single outburst scenario. Owing

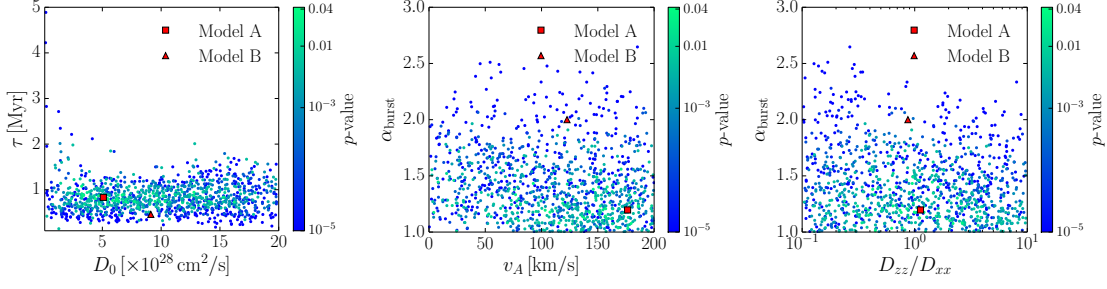


Figure 1: Scatter plots of the scan over the parameter space for the single-outburst scenario. The best-fit model is indicated by the red square (Model A), while the red triangle represents the second benchmark (Model B), i.e. the best-fit model with injected spectral index $2 < \alpha < 2.4$. In general, $\tau \sim 1$ Myr and high re-acceleration ($v_A > 100$ km/s) are required to fit well the GeV excess data. Anisotropic diffusion does not improve significantly the fit.

Parameter	Model A	Model B	Model C
α_1	1.2	2.0	1.1
α_2	NA	NA	1.0
$E_{\text{cut},1}$	1 TeV	1 TeV	20 GeV
$E_{\text{cut},2}$	NA	NA	60 GeV
τ_1 (Myr)	0.83	0.46	0.1
τ_2 (Myr)	NA	NA	1.0
N_1 (10^{51} erg)	2.89	9.87	0.1
N_2 (10^{51} erg)	NA	NA	0.88
δ	0.20	0.23	0.3
D_0 (10^{28} cm ² /s)	5.08	9.12	9.0
D_{zz}/D_{xx}	1.12	0.87	NA
v_A (km/s)	176	122	150
B_0 (μ G)	11.5	11.5	11.7
r_c (kpc)	10.0	10.0	10.0
z_c (kpc)	2.0	2.0	0.5
dv_c/dz (km/s/kpc)	0.0	0.0	0.0
ISRF	1.0, 1.0	1.0, 1.0	1.8, 0.8
χ^2 (p -value)	277 (0.04)	317 (0.0004)	261 (0.14)

Table 1: Parameter values of the single- (Model A, B) and double-outburst (Model C) benchmark models. Parameters associated with the burst properties are α , E_{cut} , τ and N , while the others are related to the CR propagation conditions (see text for details). We also quote the χ^2 (with 240 - 1 degrees of freedom) and p -values.

to the better performance of DRAGON (w. r. to the publicly available version of Galprop) in terms of memory management and computation time, we run a multi-dimensional parameter scan by using the nested sampling algorithm of MultiNest [23]. The parameters (ranges/priors) are: the diffusion coefficient D_0 in units of 10^{28} cm²/s (0.1 – 20/linear), the diffusion index δ (0.1 – 1/linear), the diffusion anisotropy coefficient D_{zz}/D_{xx} (0.1 – 10/log), the Alfvén velocity v_A (0 – 200 km/s/linear), the injection spectral index α (1 – 3/linear) and the burst age τ (0.1 – 5 Myr/linear). The cutoff is here fixed to $E_{\text{cut}} = 1$ TeV.

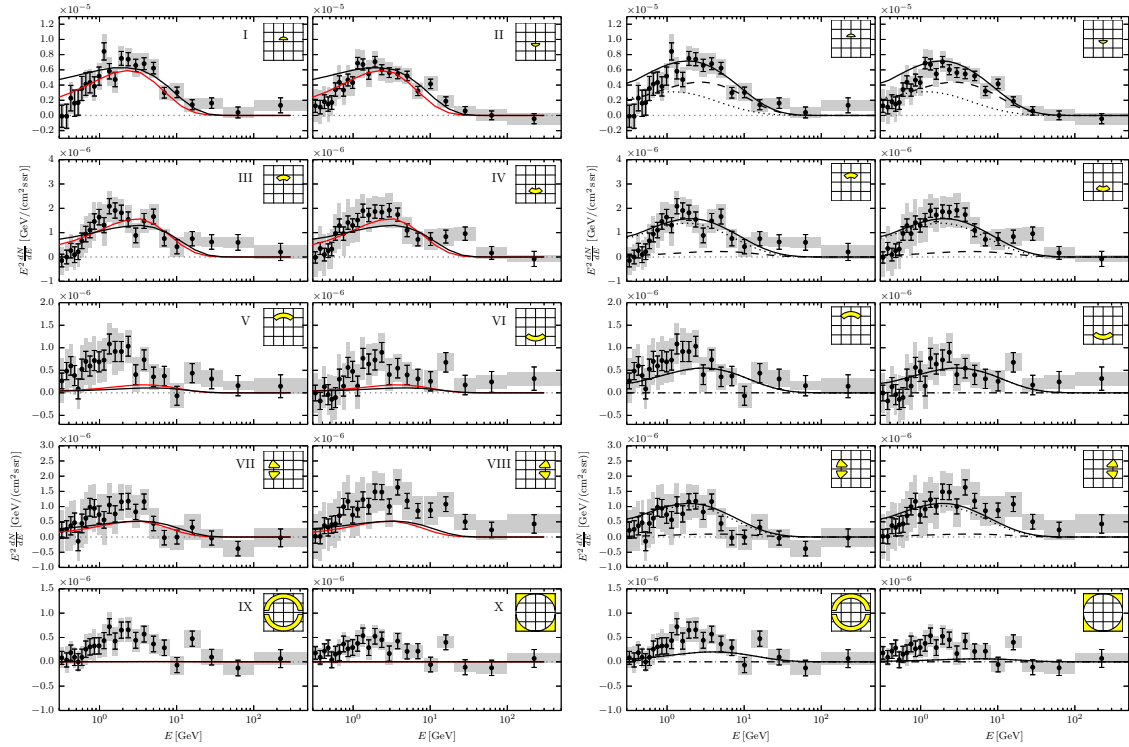


Figure 2: Left panel: GeV excess fluxes in the ten sub-regions of the analysis in Ref. [6] and expected fluxes from the single-outburst benchmark models A (red) and B (black). None of this models provides a good fit to the data (p -values of 0.04 and 0.0004, respectively), although the harder injection spectral index ($\alpha = 1.2$) of Model A improves the fit. Right panel: Same as left panel for the two-outburst benchmark, Model C. The dashed (dotted) curve represents the flux of the younger (older) outburst, while the solid line is the total model emission.

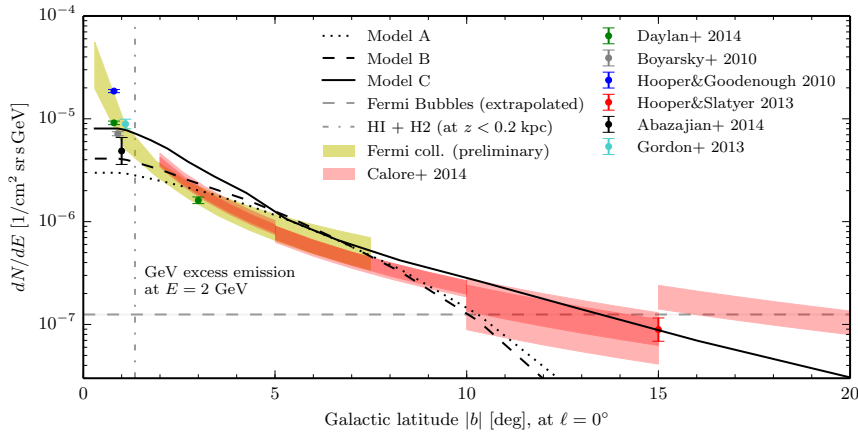


Figure 3: Angular profile of the GeV excess flux, at 2 GeV, for the single- (Model A, B) and double-outburst benchmark models (Models C). The single outburst models account for the excess morphology in the range $\sim 2^\circ - 8^\circ$, while Model C is able to fit it between $\sim 1^\circ - 15^\circ$. None of the models identified is able to account for the morphology of the excess in the inner 2° .

The best-fit found by the scan corresponds to a model with a rather hard injection spectral index ($\alpha=1.2$), age of about 1 Myr and total energy injected of a few 10^{51} erg. The CR propagation parameters preferred by the fit indicate a value for the diffusion coefficient compatible with local CR measurements, as well as the diffusion index δ , while in general high re-acceleration is required. Figure 1 shows the results of the large parameter space scan: the color bar of the scatter plots represents the p -value of the model-points explored by the scan. Burst ages of about a few Myr are preferred by the scan as well as injection spectra harder than the standard $\alpha=2$ (as predicted by Fermi acceleration). In general, the fit is not affected significantly by the choice of D_0 (since the burst age is mostly determined by the energy loss time-scale instead of the diffusion timescale), as well as by the inclusion of anisotropic diffusion, D_{zz}/D_{xx} . Instead, high re-acceleration values are preferred by the scan. We define two single-burst benchmark models: Model A is the best-fit of the parameter scan, while Model B is the best-fit corresponding to the prior $2 < \alpha < 2.4$ (as in Ref. [14]). In Table 1 we quote the parameters of the benchmark models as well as the corresponding p -values, from which one can infer that none of these models give a very good fit to the GeV excess data. Indeed, in Figure 2, left panel, we show the fluxes predicted by Model A and B in the ten sub-regions analyzed in Ref. [6], together with the observed GeV excess data. While fitting well the GeV observed data in the innermost regions (ROIs I – IV), the single-outburst benchmarks clearly fail to describe the observed fluxes in the outermost regions (ROIs V – X). Indeed the electrons cannot efficiently cool further out radially if they were required to have a significant flux in the inner 5° . We thus showed that a single leptonic outburst is not enough to explain the observed morphology of the GeV excess. This conclusion justify our decision to explore a two-outburst scenario where a younger burst, $\mathcal{O}(0.1)$ Myr, is responsible for the emission in the inner sub-regions, while an older one, $\mathcal{O}(1)$ Myr, for the emission at higher latitudes.

We again explore a large parameter space for the CR propagation conditions, allowing the ISRF normalizations and the magnetic field parameters to vary (see Ref. [1] for more details about the parameter variation). The best-fit model in the case of two outbursts shows again hard injection spectral indices for the two bursts ($\alpha_1 = 1.1$ and $\alpha_2 = 1.0$), total amount of injected energy of the order of 1×10^{50} and 9×10^{50} for the younger (0.1 Myr) and older (1 Myr) burst, respectively. The energy cutoff is $E_{\text{cut}} = 20$ GeV and 60 GeV, for the younger and older burst respectively. The cutoffs are required in order to guarantee the total gamma-ray spectrum to be approximately uniform in the whole ROI. As for the CR parameters, the best-fit two-outburst model (Model C) prefers standard value for the diffusion parameters and high re-acceleration values ($v_A \sim 150$ km/s). The p -value (0.14) for Model C is better than the one of single-burst scenario, because of the possibility to describe simultaneously the innermost and outermost sub-regions. As it can be seen from Figure 2, right panel, indeed the two-burst benchmark accounts for the emission in regions I – IV thanks to the younger burst, while it can explain the observed flux up to region IX owing to the emission from the older burst.

Finally, in Figure 3 we show the angular profile of the emission at 2 GeV as observed in the data (under the assumption of a dark matter profile with inner slope 1.26) and expected by the three benchmarks defined above. For Model C, it is evident the interplay between younger and older burst in describing the morphology of the signal from approximately 1° up to 15° , while both Model A and B can account for the morphology only in a limited angular range, between about 2° and 8° . Nonetheless, the morphology in the inner few degrees cannot be even described by the

two-outburst model.

4. Conclusions

We have systematically scrutinized the possibility that the GC GeV excess in the inner Galaxy originates from the diffuse emission of a new injected population of high-energy electrons some Myr ago. The spectrum of the GeV excess might easily be explained by the natural cutoff of the inverse Compton flux that occurs because of energy losses. However, we demonstrated that, contrary to previous findings, the morphology of the GeV excess at $|b| > 2^\circ$ cannot be explained by a single burst model, despite exploring a large parameter space. Instead, two outbursts – one older (1 Myr) and one younger (0.1 Myr) – provide a good fit to the spatial properties of the excess signal although the parameter space preferred for this model is somewhat unlikely: it requires hard spectral indices and a fine tuning of the propagation parameters, so that the predicted total spectrum appears to be uniform in the whole region of interest as suggested by the data. In particular, the values of the spectral indices are much harder than what generally predicted by first-order Fermi acceleration. Such indices are also incompatible with the observed electron injection spectra of gamma-ray blazars [24]. Still, an hardening of the injection index might result from strong diffusive re-acceleration and turbulence (that might cause the spectral cutoff from synchrotron energy losses) in the GC region. Finally, even in models with two outbursts, it is not possible to account for the spatial properties of the signal in the inner few degrees. This suggests that either an additional younger burst is required or that the dominant fraction of the signal might be due to unresolved point-sources, as recently claimed by Refs. [11, 12]. In summary, we cannot observationally rule out a series of leptonic outbursts as explanation of the GeV excess but we stress that the required features of such bursts (as for example the hard injection index) are quite extreme and make this scenario observationally viable, albeit quite unlikely.

Acknowledgements. FC is supported by the European Research Council through the ERC starting grant WIMPs Kairos, P.I. G. Bertone.

References

- [1] I. Cholis, C. Evoli, F. Calore, T. Linden, C. Weniger, et al., *The Galactic Center GeV Excess from a Series of Leptonic Cosmic-Ray Outbursts*, [arXiv:1506.05119](https://arxiv.org/abs/1506.05119).
- [2] **Fermi/LAT Collaboration** Collaboration, V. Vitale and A. Morselli, *Indirect Search for Dark Matter from the center of the Milky Way with the Fermi-Large Area Telescope*, [arXiv:0912.3828](https://arxiv.org/abs/0912.3828).
- [3] L. Goodenough and D. Hooper, *Possible Evidence For Dark Matter Annihilation In The Inner Milky Way From The Fermi Gamma Ray Space Telescope*, [arXiv:0910.2998](https://arxiv.org/abs/0910.2998).
- [4] K. N. Abazajian, N. Canac, S. Horiuchi, and M. Kaplinghat, *Astrophysical and Dark Matter Interpretations of Extended Gamma-Ray Emission from the Galactic Center*, *Phys.Rev.* **D90** (2014), no. 2 023526, [[arXiv:1402.4090](https://arxiv.org/abs/1402.4090)].
- [5] T. Daylan, D. P. Finkbeiner, D. Hooper, T. Linden, S. K. N. Portillo, et al., *The Characterization of the Gamma-Ray Signal from the Central Milky Way: A Compelling Case for Annihilating Dark Matter*, [arXiv:1402.6703](https://arxiv.org/abs/1402.6703).

- [6] F. Calore, I. Cholis, and C. Weniger, *Background model systematics for the Fermi GeV excess*, *JCAP* **1503** (2015) 038, [[arXiv:1409.0042](#)].
- [7] **Fermi-LAT** Collaboration, S. Murgia, *Observations of High-Energy Gamma-Ray Emission Toward the Galactic Center*, *Talk given at the 2014 Fermi Symposium, Nagoya, Japan, October 20-24* (2014).
- [8] F. Calore, I. Cholis, C. McCabe, and C. Weniger, *A Tale of Tails: Dark Matter Interpretations of the Fermi GeV Excess in Light of Background Model Systematics*, [arXiv:1411.4647](#).
- [9] P. Agrawal, B. Batell, P. J. Fox, and R. Harnik, *WIMPs at the Galactic Center*, [arXiv:1411.2592](#).
- [10] A. Achterberg, S. Caron, L. Hendriks, R. Ruiz de Austri, and C. Weniger, *A description of the Galactic Center excess in the Minimal Supersymmetric Standard Model*, [arXiv:1502.05703](#).
- [11] R. Bartels, S. Krishnamurthy, and C. Weniger, *Strong support for the millisecond pulsar origin of the Galactic center GeV excess*, [arXiv:1506.05104](#).
- [12] S. K. Lee, M. Lisanti, B. R. Safdi, T. R. Slatyer, and W. Xue, *Evidence for Unresolved Gamma-Ray Point Sources in the Inner Galaxy*, [arXiv:1506.05124](#).
- [13] E. Carlson and S. Profumo, *Cosmic Ray Protons in the Inner Galaxy and the Galactic Center Gamma-Ray Excess*, *Phys.Rev.* **D90** (2014) 023015, [[arXiv:1405.7685](#)].
- [14] J. Petrovic, P. D. Serpico, and G. Zaharijas, *Galactic Center gamma-ray "excess" from an active past of the Galactic Centre?*, *JCAP* **1410** (2014), no. 10 052, [[arXiv:1405.7928](#)].
- [15] G. Dobler, D. P. Finkbeiner, I. Cholis, T. R. Slatyer, and N. Weiner, *The Fermi Haze: A Gamma-Ray Counterpart to the Microwave Haze*, *Astrophys.J.* **717** (2010) 825–842, [[arXiv:0910.4583](#)].
- [16] M. Su, T. R. Slatyer, and D. P. Finkbeiner, *Giant Gamma-ray Bubbles from Fermi-LAT: AGN Activity or Bipolar Galactic Wind?*, *Astrophys.J.* **724** (2010) 1044–1082, [[arXiv:1005.5480](#)].
- [17] **Fermi-LAT Collaboration** Collaboration, M. Ackermann et al., *The Spectrum and Morphology of the Fermi Bubbles*, *Astrophys.J.* (2014) [[arXiv:1407.7905](#)].
- [18] A. W. Strong and I. V. Moskalenko, *Propagation of cosmic-ray nucleons in the Galaxy*, *Astrophys. J.* **509** (1998) 212–228, [[astro-ph/9807150](#)].
- [19] G. Di Bernardo, C. Evoli, D. Gaggero, D. Grasso, and L. Maccione, *Unified interpretation of cosmic-ray nuclei and antiproton recent measurements*, *Astropart.Phys.* **34** (2010) 274–283, [[arXiv:0909.4548](#)].
- [20] C. Evoli, D. Gaggero, D. Grasso, and L. Maccione, *Cosmic-Ray Nuclei, Antiprotons and Gamma-rays in the Galaxy: a New Diffusion Model*, *JCAP* **0810** (2008) 018, [[arXiv:0807.4730](#)].
- [21] <http://galprop.stanford.edu/>.
- [22] G. Blumenthal and R. Gould, *Bremsstrahlung, synchrotron radiation, and compton scattering of high-energy electrons traversing dilute gases*, *Rev.Mod.Phys.* **42** (1970) 237–270.
- [23] F. Feroz, M. Hobson, E. Cameron, and A. Pettitt, *Importance Nested Sampling and the MultiNest Algorithm*, [arXiv:1306.2144](#).
- [24] M. Boettcher, A. Reimer, K. Sweeney, and A. Prakash, *Leptonic and Hadronic Modeling of Fermi-Detected Blazars*, *Astrophys.J.* **768** (2013) 54, [[arXiv:1304.0605](#)].